HHS Public Access

Author manuscript

J Occup Environ Med. Author manuscript; available in PMC 2015 December 15.

Published in final edited form as:

J Occup Environ Med. 2012 August ; 54(8): 1010–1016. doi:10.1097/JOM.0b013e318255ba74.

Characterization of Frequency-Dependent Responses of the Vascular System to Repetitive Vibration

Kristine Krajnak, PhD, **G. Roger Miller, BS**, **Stacey Waugh, MS**, **Claud Johnson, BS**, and **Michael L. Kashon, PhD**

Engineering and Controls Technology Branch (Dr Krajnak, Mr Miller, Ms Waugh, and Mr Johnson) and Biostatics and Epidemiology Branch (Dr Kashon), National Institute for Occupational Safety and Health, Health Effects Laboratory Division, Morgantown, WVa

Abstract

Objective—Occupational exposure to hand-transmitted vibration can result in damage to nerves and sensory loss. The goal of this study was to assess the frequency-dependent effects of repeated bouts of vibration on sensory nerve function and associated changes in nerves.

Methods—The tails of rats were exposed to vibration at 62.5, 125, or 250 Hz (constant acceleration of 49m/s^2) for 10 days. The effects on sensory nerve function, nerve morphology, and transcript expression in ventral tail nerves were measured.

Results—Vibration at all frequencies had effects on nerve function and physiology. However, the effects tended to be more prominent with exposure at 250 Hz.

Conclusion—Exposure to vibration has detrimental effects on sensory nerve function and physiology. However, many of these changes are more prominent at 250-Hz exposure than at lower frequencies.

Hand-arm vibration syndrome (HAVS) is caused by repeated exposure to vibration through the use of powered and pneumatic hand tools.[1] The hallmark symptom of HAVS is cold-induced vasospasms that result in finger blanching. However, sensorineural deficits in the fingers and hands are also prevalent in workers with HAVS.[2] These deficits include reductions in tactile and heat sensitivity and a loss of manual dexterity. In addition, workers with HAVS also develop hand and finger pain, particularly when exposed to cold.[3] Biopsy samples collected from the fingers of workers diagnosed with HAVS have demonstrated that these changes in sensorineural function are associated with a loss of peripheral nerves, nerve fibrosis, and demyelination.[4,5] Even though the morphologic and functional changes associated with sensory loss in workers with HAVS have been characterized, the mechanisms by which vibration causes these changes are still not well understood.

One factor that is believed to affect the risk of injury is the vibration frequency or frequencies to which a worker is exposed. Currently, the International Standards

Address correspondence to: Kristine Krajnak, PhD, NIOSH, 1095 Willowdale Rd, MS2027, Morgantown, WV 26505 (ksk1@cdc.gov).

None of the authors have any conflicts of interest with regards to this research.

Organization (ISO) standard ISO 5349-1[6] presents a weighting curve that predicts the risk of developing a vibration-induced injury. One of the factors used to calculate the weighting factor is the dominant frequency to which a worker is exposed. This weighting curve assigns significantly greater weighting to low-frequency vibration (ie, ≤16 Hz), and the weighting dramatically decreases with exposures greater than 100 Hz. However, experimental and epidemiologic studies suggest that vibration-induced injuries to the fingers and hands may actually be more prevalent in workers using tools that emit a higher-frequency vibration.[7–9] It has been hypothesized that the increased risk of injury associated with exposure to higher frequencies may be because stress and strain to the soft tissues of the fingers and hands is greatest with exposure to frequencies between 100 and 300 Hz.[10,11] However, few studies have been able to assess the frequency exposure–response relationship between vibration and injury or dysfunction.

The goal of this study was to use a rat tail model characterized in our laboratory[12] to examine the frequency-dependent responses of sensorineural function, peripheral nerves, and sensory neurons in the dorsal root ganglia (DRG) to vibration. We have previously used this model to characterize frequency-dependent changes in vascular function and identify some of the mechanisms that may underlie these changes.[13] In this study we exposed the tails of rats to vibration to test the hypothesis that vibration-induced disruption of the sensorineural system would be greatest with exposure to vibration at frequencies that induce the greatest tissue stress and strain (ie, between 125 and 250 Hz).[12] We previously demonstrated that vibration exposure at 125 Hz results in a transient decrease in the sensitivity of large, myelinated Aβ fibers to transcutaneous electrical stimulation using the current perception threshold (CPT) test.[14] In this study, we also assessed the effects of exposure to different vibration frequencies on the sensitivity of Aβ fibers to electrical stimulation. In addition, we tested rats for changes in sensitivity to mechanical stimulation by using von Frey filaments. Changes in myelin thickness, myelinated axon number, inflammation, and edema were also assessed in the ventral tail nerves. In addition, transcript expression in the DRG and ventral tail nerves were measured to determine whether changes in function were associated changes in transcript expression. We specifically looked for changes in markers for myelin injury and repair (nerve), inflammation (nerve and DRG), and oxidative stress (DRG) because pilot data collected using gene arrays indicated that vibration might affect these processes in these tissues.

METHODS

Animals

Male Sprague-Dawley rats [Hla:(SD) CVF] (Hilltop Lab Animals, Inc, Scottdale, PA) that were 6 weeks of age at arrival were used in both studies. Rats were maintained in a colony room with a 12:12 light–dark cycle (lights on at 7:00 AM) and with Teklad 2918 food and tap water available ad libitum, at the National Institute for Occupational Safety and Health facility, which is accredited by the Association for Assessment and Accreditation of Laboratory Animal Care. Rats were acclimated to the facilities for 1 week before being used in experiments. All procedures were approved by the National Institute for Occupational Safety and Health Animal Care and Use Committee and were in compliance with the Public

Health Service Policy on Humane Care and Use of Laboratory Animals and the National Research Council Guide for the Care and Use of Laboratory Animals.

Vibration Exposures

The equipment and protocol for exposing animals to vibration previously have been described.[13,15] Briefly, vibration and restraint-control rats were restrained in Broome-style restrainers. Each vibrated rat's tail was secured to a vibrating platform that was attached to a shaker and rats were exposed to 4-hour bouts of vibration (62.5, 125, or 250 Hz; acceleration of 49 m/s^2 root mean squared; $n = 8$ rats/frequency) between 9:00 AM and 1:00 PM each day for 10 consecutive days. Restraint-control rats were treated in an identical manner except that their tails were secured to nonvibrating platforms mounted on isolation blocks. Cage-control rats were maintained in their home cages in the colony room during exposures.

Current Perception Thresholds and Mechanical Sensitivity Testing

On days 1 and 9 of the study, each rat was placed in a Broome-style restrainer before the exposure, and CPT measurements were made using a Neurometer CPT/C (Neurotron, Inc, Baltimore, MD). We chose to assess rats on day 9 instead of day 10 so that the functional tests would not interfere with biological measures. The CPT was performed as described by Krajnack et al.[14] In brief, each rat was put into a sound-attenuated chamber, and its tail was cleaned with Goldtrobe electrode preparation paste and wiped with an alcohol pad. Goldtrobe electrode gel was applied to the stimulating electrode (ATE1925), and the electrode was secured to the ventral surface of the tail, just distal to the C15 tail vertebrae, using Soft-Tape (Neurotron, Inc). A separate skin patch dispersion electrode (SDE44; Neurotron, Inc) was secured on the tail approximately 2 cm proximal to the stimulating electrode.

Transcutaneous electrical stimulation at a frequency of 2000 Hz was used to assess the function of large, myelinated Aβ nerve fibers. The test was started with a stimulus of 10 mA, and the intensity of the stimulus was automatically increased in increments of 1.0 mA until the rat flicked its tail. The intensity that elicited the tail flick was recorded as the CPT. A single CPT test was performed at all three frequencies and then there was a 1-minute rest interval before repeating the test. The CPT test set was repeated two additional times. CPTs were measured immediately prior to vibration or restraint-control exposures. Cage-control rats were tested at the same times. The mean CPTs were calculated on each day and used for statistical analysis.

von Frey filaments were used to assess mechanical sensitivity immediately following the CPT test. Each rat's tail was laid on a wire grid. Sensitivity was tested by gently pressing a 1-, 10-, or 60-g filament against the ventral surface of the C15 region of the tail. Animals were tested with each filament in ascending order and then given a 1-minute rest interval. The test was repeated three times. If an animal flicked its tail before the filament bent, it was counted as a positive response. Rats that responded to a specific filament in two out of three trials were labeled as sensitive to that stimulus.

Tissue Samples

One hour after the final exposure, rats were deeply anesthetized with pentobarbital (100 mg/kg, intraperitoneally), and killed by exsanguination. Nerves from the C13 to C15 region of the tail and DRG from the L4 to C5 region of the left side were stored in cryovials, immediately frozen in liquid nitrogen, and stored at −80°C until used for quantitative reverse transcription-polymerase chain reaction (PCR). Nerves from the right side were embedded in Tissue Tek mounting media and frozen for immunohistochemisty. The C17 to C18 segments of each rat's tail were placed in 15-mL conical tubes and immersion fixed overnight using 4%paraformaldehyde + 0.1M phosphate buffer (pH 7.3). The next morning the ventral tail nerves were dissected from the fixed segments and placed in 2-mL cryovials containing 1.5 mL of 10 mM phosphate-buffered saline. Vials were stored at 4°C until processed for morphologic analyses.

We chose to assess nerves from these specific regions of the tail because we have demonstrated that the physical stress and strain of vibration is greatest in these regions[12] and ventral tail arteries from these regions display altered responses to vasoconstricting and vasodilating factors after exposure to 10 days of vibration.[13,15]

Quantitative Reverse Transcription Polymerase Chain Reaction

Quantitative reverse transcription PCR was used to identify changes in transcripts in nerve and DRG samples using previously described methods.[16] The transcripts examined and all primer sequences are presented in Table 1. Briefly, RNA was isolated and purified and first-strand complementary DNA was synthesized from 1 εg of total RNA using Invitrogen's Reverse Transcription System (Invitrogen, Carlsbad, CA). Samples that did not show a single defined melt peak in the 80°C range were not included in the data set. Fold changes from control were calculated for each transcript and used for analyses.

Morphologic Analysis

Fixed nerve samples were dehydrated at room temperature with agitation using increasing concentrations of ethanol. Dehydrated samples were embedded using a JB4 Embedding Kit (Electron Microscopy Sciences, Hatfield, PA) following the manufacturer's instructions. Briefly, samples were incubated in JB4 Infiltration solution at 4°C overnight with agitation. The next morning fresh solution was added, and after 4 hours of incubation, nerves were removed and placed in 2 × 15 × 5 mm molding trays (Electron Microscopy Sciences). Embedding solution (1.2 mL) was added to each mold. Samples were allowed to polymerize on the bench at room temperature overnight.

Nerve sections (2 εm) were cut on a Sorvall JB4 Microtome. Four sections were wet mounted on each microscope slide and dried at 60°C for 5minutes. Slides were stained using freshly prepared and filtered 0.25% Sudan Black B in 70% ethanol stain, washed, dried briefly at 37°C, and cover slipped with Permount (Fisher Scientific, Pittsburgh, PA). Sections were viewed on an Olympus microscope (model no. AX70TRF, Waltham, MA) equipped with 100×/1.35 Oil Iris UPlanApo objective. Images were obtained by a SPOT camera and SPOT Advanced Version 4.6.4.6/4.7.5.2 software (Diagnostic Instruments, Inc, Sterling Heights, MI). To assess the number of myelinated fibers and myelin thickness, each

nerve section (3 to 4 sections/rat) was centered in the field of view; four fields around the center (one to the top and bottom and one to each side) were identified and fiber number and thickness were measured in all nerves in that field. To measure the thickness, the perimeter directly inside and outside the stained myelin was measured, and the internal perimeter was subtracted from the external perimeter. An average myelin thickness from all nerves analyzed in each animal was calculated and used for analyses.

Immunohistochemistry

Sections (10 εm) were cut in a cryostat, thaw-mounted onto slides, and stored at −20°C until processed by albumin immunohistochemistry using a previously published protocol.[13] The primary antibody was rabbit anti-albumin (Santa Cruz Biotech Inc, Santa Cruz, CA) and was used at a final dilution of 1:67, and the secondary antibody was Cy3-labeled donkey anti-rabbit immunoglobulin G (Jackson Immunolabs, West Grove, PA), used at a final dilution of 1:500. All antibodies were diluted in phosphate-buffered saline containing 0.4% Triton-x 100. Nerve sections (3 to 4 section/animal; 100 εm between consecutive sections) were centered under the objective, and images from the middle of each nerve section were captured using a Zeiss LSM510 confocal microscope at a final magnification of 45× and ZEN software (Zeiss International, Inc, Thornwood, NY). ImageJ software (National Institutes of Health, Bethesda, MD) was used to measure the density of albumin staining in each image. Briefly, a threshold and light level were set and the area of each image that was above threshold was measured. The area measures were averaged for analyses.

Statistical Analyses

Fold changes in transcript levels, immunostained area of the nerves, and morphologic data (myelinated nerve number and myelin thickness) were analyzed using one-way analyses of variance. CPTs were analyzed using two-way interaction (treatment × day), with animal being treated as a random variable. Tukey tests were used for all pairwise comparisons where appropriate. The von Frey data were analyzed using Wilcoxon ranked sum nonparametric statistics to compare the number of rats responding to each filament at each time point and were used to perform pairwise comparisons. Differences with $P < 0.05$ were considered significant unless otherwise noted.

RESULTS

CPTs and Mechanosensitivity

Thresholds to transcutaneous electrical stimulation measured at all three frequencies are presented in Fig. 1A. There was a significant interaction between frequency and day of exposure ($F_{4,20} = 5.13$; $P < 0.05$). Prior to vibration exposure (day 1), thresholds in all groups of rats were similar. There was a significant reduction in CPTs between days 1 and 9 (ie, increase in sensitivity to electrical stimulation) in rats exposed to vibration at all frequencies. On day 9 of the study, rats exposed to vibration at 62.5, 125, and 250 Hz also displayed significant reductions in CPTs when compared with cage-control rats, restraint-control rats, and rats exposed to vibration. Although day-9 CPTs seemed to be lower in rats exposed to vibration at 250 Hz than in rats exposed to vibrations at 62.5 or 125 Hz, these differences were not significant.

When rats were tested using the von Frey filaments, all animals displayed positive responses to the 60-g filament, but no rats responded to touch with the 1-g filament (data not shown). However, group differences were seen using the 10-g filament (Fig. 1B). On day 1, one or two rats in each group showed a positive response (tail flick) to touch with the 10-g filament. However, the number of rats responding to stimulation with the 10-g filament significantly increased from day 1 to day 9 of the study among those exposed to 250 Hz. In addition, the number of rats responding to the 10-g filament was higher in the 250-Hz group than in the cage- or restraint-control groups. However, there were no significant effects of vibration frequency on the number of responses on day 9.

Morphology and Immunohistochemistry

The number of myelinated axons did not differ between groups of rats (Fig. 2A), but myelin thickness was reduced in rats exposed to vibration at 250 Hz when compared with cage- and restraint-control rats (Fig. 2B). The organization of the axons within the ventral tail nerve also seemed to be disrupted in rats exposed to vibration at 250 Hz, and albumin staining was significantly greater in nerves from rats exposed to vibration at 250 Hz than in cage- and restraint-control rats and rats exposed to vibration at 62.5 Hz (Fig. 2C).

Quantitative Polymerase Chain Reaction

In the ventral tail nerves, expression for a growth factor, glial-derived neurotrophic factor (GDNF), was generally greater in rats exposed to vibration than in cage- or restraint-control rats. Expression for the proinflammatory factor monocyte chemoattractant protein (MCP)-1 was also greater in rats exposed to vibration at 125 Hz than in restraint-control rats and in rats exposed to vibration at 250 Hz (Fig. 3A and B). Changes in transcript expression in the DRG are presented in Table 2. Transcript levels for cadherin-2, Keap, mitogen-activated protein kinase (MAPK) 8, platelet activating factor, postsynaptic density 96, superoxide disumatase (SOD) 1, and SOD-2 were greater in rats exposed to 250 Hz than in cage-control rats. Transcript levels for glutathione synthetase were higher in rats exposed to 250 Hz than in cage- or restraint-control rats. Restraint-control rats and rats exposed to vibration at 250 Hz also had lower levels of signal transducer and activator of transcription 3 expression and higher levels of MAPK-8 expression in the DRG than cage-control rats.

DISCUSSION

The current ISO 5349 standard contains a weighting curve to help workers predict the risk of injury.[6] The assigned weighting is significantly reduced at frequencies greater than 16 Hz, thereby resulting in little weight being given to exposures to frequencies greater than 100 Hz. Although the development of HAVS has been linked to exposure to a wide range of vibration frequencies, including low-range frequencies (ie, less than 30 Hz), studies in humans have suggested that exposure to vibration at or near the resonant frequency of the finger-hand system (ie, 100 to 300 Hz, depending on the location of the measurement) may pose the greatest risk for inducing peripheral vascular and nerve damage.[7,17] It has been hypothesized that the increased risk of injury with exposure to these frequencies could be because local stress and strain on the soft tissues is greatest with these exposures.[11] Studies assessing the physical or biodynamic effects of vibration on rat tails suggest that the tail can

be used as a model to assess mid-range frequencies (ie, 60 to 300 Hz), but the tail does not serve as a good model for assessing the effects of vibration at lower frequencies.[12] Because of the current questions regarding the effects of mid-range frequencies, and because the rat tail does not serve as a good model for examining the effects of lower frequencies, we chose to assess only the effects of vibration on mid-range frequencies, and thus our results do not address the risk of nerve damage associated with low-frequency exposures.

We have demonstrated that tissue stress and strain in our model of vibration-induced injury occurs at approximately 250 Hz (depending on the precise location where the measurement was taken[12] and that exposure to vibration at this frequency induces vascular dysfunction more quickly than exposure to frequencies that induces less local stress and strain.[13] The results of this study suggest that vibration-induced changes in peripheral nerve function and morphology are frequency dependent in the 60 to 300 Hz range, but nerves may be more sensitive than vascular tissues to vibration exposure, and injuries and dysfunction may occur over a wider range of frequencies.

In this study, rats exposed to vibration at 62.5, 125, and 250 Hz displayed a reduction in CPTs on day 9 of exposure (ie, an increase in sensitivity to stimulation). However, only exposure to vibration at 250 Hz resulted in an increase in the number of rats responding to mechanical stimulation with a 10-g von Frey filament. The CPT uses transcutaneous electrical stimulation to directly stimulate nerves, and it bypasses activation of sensory receptors located in the skin.[18] Electrical stimulation at 2000 Hz preferentially stimulates myelinated Aβ fibers. These fibers primarily carry sensory information from mechanoreceptors to the central nervous system.[19] In contrast, responses to stimulation with the von Frey filaments depend upon the response of local mechanoreceptors in the skin and Aβ fiber function. Workers with HAVS normally display a reduced sensitivity to mechanical stimuli after years of exposure.[20] This reduction in sensitivity is associated a reduction in innervation in the skin.[5,21] Studies examining more acute effects of nerve injury induced by compression or chemical injection have shown that nerve injury can initially induce hyperalgesia.[22,23] In the current study, we did not see a reduction in the number of myelinated axons in the ventral tail nerve. However, rats exposed to vibration at 250 Hz did display a reduction in myelin thickness and an increase in albumin staining, which is indicative of edema. These morphologic changes certainly could underlie functional changes seen in these rats. However, rats exposed to vibration at 62.5 and 125 Hz also displayed reduced CPTs, but these changes were not associated with changes in myelin thickness or edema. It is possible that the injury induced by exposure at these frequencies was not as severe after 8 days of exposure or that other physiologic changes underlie the reduction in CPTs seen in these rats (eg, changes in ion channel numbers[24]. Additional studies examining other potential mechanisms and longer exposures may be needed to address these issues.

Changes in function and peripheral nerve morphology also were associated with an increase in transcript levels for the growth factor GDNF in nerves of all rats exposed to vibration. GDNF can be produced by Schwann cells and helps stimulate nerve regrowth and repair after an injury.[25,26] The increase in GDNF seen in the nerves from vibrated rats is consistent with the idea that vibration exposure at all frequencies resulted in damage to ventral tail

nerves. Exposure to vibration also resulted in an increase in MCP-1, but this increase was seen only in nerves from rats exposed to vibration at 125 Hz. MCP-1 is produced by infiltrating macrophages and is involved in stimulating pathways that regulate the removal of debris and regeneration.[27] Increases in the expression of MCP-1 and other proinflammatory factors such as tumor necrosis factor α and interleukin 1β have been associated with nerve injury, but the changes are transient and occur at varying time points after nerve injury.[28] Thus, we may have missed vibration-induced changes in the other proinflammatory factors because we assessed only transcript expression at a single time point after exposure. Studies examining additional time points may provide a more complete picture of the inflammatory response generated by vibration exposure.

We also examined the effect of vibration on transcript expression in the DRG. Pilot work using gene arrays suggested that vibration might induce changes in factors associated with inflammation and oxidative stress. In models of diabetic neuropathy, there is an increased expression of factors involved in oxidative activity in the DRG, and an increase in oxidative activity has been associated with peripheral nerve death.[29–31] Increases in these factors may be because of the activation of local microglia and are associated with the development of neuropathic pain.[32,33] Although we did not directly assess oxidative activity in the DRG, our PCR data from the ganglia are consistent with these findings; exposure to vibration resulted in increases in the expression of platelet activating factor, SOD-1, SOD-2, glutathione synthetase, and glutathione peroxidase in the DRG, and these increases were most prominent in tissue from rats exposed at 250 Hz. If maintained over time, increases in oxidative activity could contribute to the sensory nerve loss seen in animals and workers exposed to vibration.

The pathways involved in the development of neuropathic pain are not fully understood, but there is evidence that inflammatory factor–induced changes in MAPK signaling may contribute to increases in oxidative activity in the DRG and spinal cord, and this could result in pain and sensory nerve degeneration.[29,34–36] Compared with cage-control rats, rats in all other groups displayed an increase in MAPK-8 and decrease in STAT3 expression in the DRG. However, these changes were only significant in the restraint-control rats and rats exposed to vibration at 250 Hz. Ischemia-induced stress has been shown to affect MAPK signaling in neurons.[37] It is possible that tail restraint and maintaining a stable position of the tail resulted in some mild ischemia[38] and thus resulted in changes in the expression of factors involved in MAPK signaling in all rats that had undergone tail restraint. Because changes in these signaling factors were not associated with alterations in morphology or differences in CPTs or responses to the von Frey filaments in restraint-control rats and rats exposed to vibration at 62.5 or 125 Hz, it seems unlikely that they were the result of any significant nerve injury.

In conclusion, the results of this study are consistent with the hypothesis that exposure to vibration at or near the resonant frequency results in greater disruption of sensory nerve physiology and structure than exposure to vibration at lower frequencies.[39] Our previous study examining frequency-dependent changes in vascular function show a clear increase in vibration-induced dysfunction with exposure to vibration near the resonant frequency of the tail (ie, approximately 250 Hz.[13] Changes in nerve physiology and markers of nerve injury

seem to occur at a broader range of frequencies; however, for the most part, these changes seem to be more prominent with exposure to vibration at 250 Hz. The resonant frequency of the human finger is also in the range of 100 to 300 Hz,[40] and thus exposure to these higher frequencies through the use of powered hand tools can induce injury. Although additional studies need to be performed, the results of this study are consistent with the idea that the current ISO 5349 standard underestimates the risk of injury associated with exposure to vibration at frequencies greater than 100 Hz.[7,9]

Acknowledgments

This research was funded by the Health Effects Laboratory Division at the National Institute for Occupational Safety and Health.

The findings and conclusions in this report are those of the authors and do not necessarily represent the views of the National Institute for Occupational Safety and Health.

REFERENCES

1. Bernard B, Nelson N, Estill CF, Fine L. The NIOSH review of hand-arm vibration syndrome: vigilance is crucial. J Occup Environ Med. 1998; 40:780–785. [PubMed: 9777561]
2. Bovenzi M. Exposure-response relationship in the hand-arm vibration syndrome: an overview of current epidemiology research. Int Arch Occup Environ Health. 1998; 71:509–519. [PubMed: 9860158]
3. Brammer AJ, Taylor W, Lundborg G. Sensorineural stages of the hand-arm vibration syndrome. Scand J Work Environ Health. 1987; 13:279–283. [PubMed: 3324308]
4. Takeuchi T, Futatsuka M, Imanishi H, Yamada S. Pathological changes observed in the finger biopsy of patients with vibration-induced white finger. Scand J Work Environ Health. 1986; 12:280–283. [PubMed: 3775312]
5. Takeuchi T, Takeya M, Imanishi H. Ultrastructural changes in peripheral nerves of the fingers of three vibration-exposed persons with Raynaud's phenomenon. Scand J Work Environ Health. 1988; 14:31–35. [PubMed: 3353694]
6. International Organization for Standardization. Mechanical Vibration – Measurement and Evaluation of Human Exposure to Hand-Transmitted Vibration – Part 1: General Requirements. ISO 5349-1. Geneva, Switzerland: International Organization for Standardization; 2001.
7. Griffin MJ, Bovenzi M, Nelson CM. Dose-response patterns for vibration-induced white finger. Occup Environ Med. 2003; 60:16–26. [PubMed: 12499452]
8. Wu JZ, Welcome DE, Krajnak K, Dong RG. Finite element analysis of the penetrations of shear and normal vibrations into the soft tissues in a fingertip. Med Eng Physics. 2007; 29:718–727.
9. Dong RG, Welcome DE, McDowell TW, Wu JZ, Schopper AW. Frequency weighting derived from power absorption of fingers-hand-arm system under zh-axis. J Biomech. 2006; 39:2311–2324. [PubMed: 16154576]
10. Dong RG, Welcome DE, McDowell TW, Wu JZ. Biodynamic response of human fingers in a power grip subjected to a random vibration. J Biomech Eng. 2004; 126:447–457. [PubMed: 15543862]
11. Wu JZ, Krajnak K, Welcome DE, Dong RG. Analysis of the dynamic strains in a fingertip exposed to vibrations: correlation to the mechanical stimuli on mechanoreceptors. J Biomech. 2006; 39:2445–2456. [PubMed: 16168999]
12. Welcome DE, Krajnak K, Kashon ML, Dong RG. An investigation on the biodyamic foundation of a rat tail model. Proc Inst Mech Eng H. 2008; 222:1127–1141. [PubMed: 19024160]
13. Krajnak K, Miller GR, Waugh S, Johnson C, Li S, Kashon ML. Characterization of frequency-dependent response of the vascular system to repetitive vibration. J Occup Environ Med. 2010; 52:584–594. [PubMed: 20523237]

14. Krajnak K, Waugh S, Wirth O, Kashon ML. Acute vibration reduces Aβ nerve fiber sensitivity and alters gene expression in the ventral tail nerves of rats. Muscle Nerve. 2007; 36:197–205. [PubMed: 17541999]
15. Krajnak K, Dong RG, Flavahan S, Welcome DE, Flavahan NA. Acute vibration increases α_{2c}-adrenergic smooth muscle constriction and alters thermosensitivity of cutaneous arteries. J Appl Physiol. 2006; 100:1230–1237. [PubMed: 16339346]
16. Krajnak K, Waugh S, Miller R, et al. Proapoptotic factor Bax is increased in satellite cells in the tibialis anterior muscles of old rats. Muscle Nerve. 2006; 34:720–730. [PubMed: 16967487]
17. Dong RG, McDowell TW, Welcome DE. Biodynamic response at the palm of the human hand subjected to a random vibration. Ind Health. 2005; 43:241–255. [PubMed: 15732329]
18. Weseley SA, Sadler B, Katims JJ. Current perception: preferred test for evaluation of peripheral nerve integrity. ASAIO Trans. 1988; 34:188–193. [PubMed: 3196507]
19. Kiso T, Nagakura Y, Toya T, et al. Neurometer measurement of current stimulus threshold in rats. J Pharmacol Exp Ther. 2001; 297:352–356. [PubMed: 11259562]
20. Bovenzi M. Health risks from occupational exposures to mechanical vibration. Med Lav. 2006; 97:535–541. [PubMed: 17009691]
21. Goldsmith PC, Molina FA, Bunker CB, et al. Cutaneous nerve fibre depletion in vibration white finger. J R Soc Med. 1994; 87:377–381. [PubMed: 8046721]
22. Gilchrist HD, Allard BL, Simone DA. Enhanced withdrawal responses to heat and mechanical stimuli following intraplantar injection of capsaicin in rats. Pain. 1996; 67:179–188. [PubMed: 8895246]
23. Dahlin LB, Danielsen N, Ehira T, Lundborg G, Rydevik B. Mechanical effects of compression of peripheral nerves. J Biomech Eng. 1986; 108:120–122. [PubMed: 3724098]
24. Huang H-L, Cendan C-M, Roza C, et al. Proteomic profiling of neuromas reveals alterations in protein composition and local protein composition in hyperexcitable nerves. Mol Pain. 2008; 4:33–47. [PubMed: 18700027]
25. Hammarberg H, Piehl F, Cullheim S, Fjell J, Hokfelt T, Fried K. GDNF mRNA in Schwann cells and DRG satellite cells after chronic sciatic nerve injury. Neuroreport. 1996; 7:857–860. [PubMed: 8724660]
26. Frostick SP, Yin Q, Kemp GJ. Schwann cells, neurotrophic factors, and peripheral nerve regeneration. Microsurgery. 1998; 18:397–405. [PubMed: 9880154]
27. Perrin FE, Lacroix S, Aviléś-Trigueros M, David S. Involvement of monocyte chemoattractant protein-1, macrophage inflammatory protein-1a and interleukin-1b in Wallerian degeneration. Brain. 2005; 128:854–866. [PubMed: 15689362]
28. Kobayashi H, Chattopadhyay S, Kato K, et al. MMPs initiate Schwann cell-mediated MBP degradation and mechanical nociception after nerve damage. Mol Cell Neurosci. 2008; 39:619–627. [PubMed: 18817874]
29. Fischer LR, Glass JD. Oxidative stress induced by loss of Cu,Zn-superoxide dismutase (SOD1) or superoxide-generating herbicides causes axonal degeneration in mouse DRG cultures. Acta Neuropathol. 2010; 119:249–259. [PubMed: 20039174]
30. Hong S, Agresta L, Guo C, Wiley JW. The TRPV1 receptor is associated with preferential stress in large dorsal root ganglion neurons in early diabetic sensory neuropathy. J Neurochem. 2008; 105:1212–1222. [PubMed: 18182051]
31. Vincent AM, Hayes JM, McLean LL, Vivekanandan-Giri A, Pennathur S, Feldman EL. Dyslipidemia-induced neuropathy in mice. The role of oxLDL/LOX-1. Diabetes. 2009; 58:2376–2385. [PubMed: 19592619]
32. Gao Y-J, Zhang L, Samad OA, et al. JNK-induced MCP-1 production in spinal cor astrocytes contributes to central sensitization and neuro-pathic pain. J Neurosci. 2009; 29:4096–4108. [PubMed: 19339605]
33. Guo W, Wang HP, Watanabe M, et al. Glial-cytokine-neuronal interactions underlying the mechanisms of persistent pain. J Neurosci. 2007; 27:6006–6018. [PubMed: 17537972]
34. Ibi M, Matsuna K, Shiba D, et al. Reactive oxygen species derived from NOX1/NADPH oxidase enahce inflammatory pain. J Neurosci. 2008; 28:9486–9494. [PubMed: 18799680]

35. Katasura H, Obata K, Miyoshi K, et al. Transforming growth factor-activated kinase 1 induced in spinal astrocytes contributes to mechanical hypersensitivity after nerve injury. Glia. 2008; 56:723–733. [PubMed: 18293403]

36. Dubovy P, Klusakova I, Svizenska I, Brazda V. Satellite glial cells express IL-6 and corresponding signal-transducing receptors in the dorsal root ganglia of rat neuropathic pain model. Neuron Glial Biol. 2010; 6:73–83.

37. Tian D, Litvak V, Lev S. Cerebral ischemia and seizures induce tyrosine phosphorylation of PYK2 in neurons and microglial cells. J Neurosci. 2000; 20:6478–6487. [PubMed: 10964954]

38. Lundborg G. Intraneural microcirculation. Orthop Clin North Am. 1988; 19:1–12. [PubMed: 3275919]

39. Dong RG, Welcome DE, Wu JZ. Frequency weightings based on biodynamics of fingers-hand-arm system. Ind Health. 2005; 43:516–526. [PubMed: 16100928]

40. Dong RG, Welcome DE, Wu JZ. Estimation of biodynamic forces distributed on the fingers and the palm exposed to vibration. Ind Health. 2005; 43:485–494. [PubMed: 16100925]

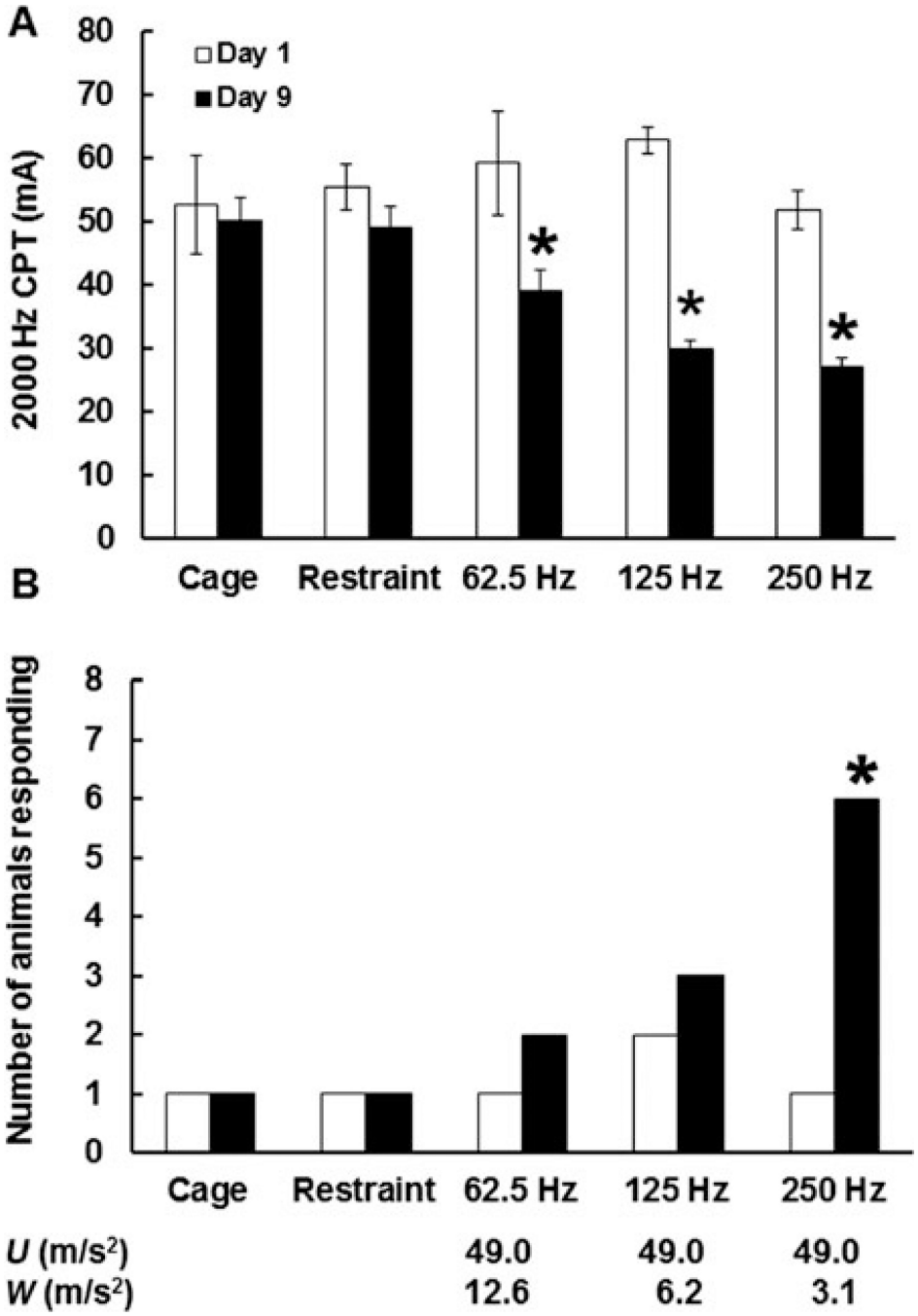

FIGURE 1.

Frequency-dependent effects of vibration on 2000 Hz current perception thresholds (CPTs) (A) and responses to stimulation with a 10-g von Frey filament (B). On day 9 of exposure, CPTs were lower in rats exposed to vibration than in cage- or restraint-control rats. Rats exposed to vibration also displayed a significant reduction in CPTs between day 1 and day 9 of exposure. However, only exposure to vibration at 250 Hz resulted in an increase in the number of rats responding to stimulation with the von Frey filament. *Less than cage- and

restraint-control rats and less than day 1 measurements, $P < 0.05$. The *x* axis shows both the un-weighted acceleration (*U*) and the ISO-weighted (*W*) acceleration for each frequency.

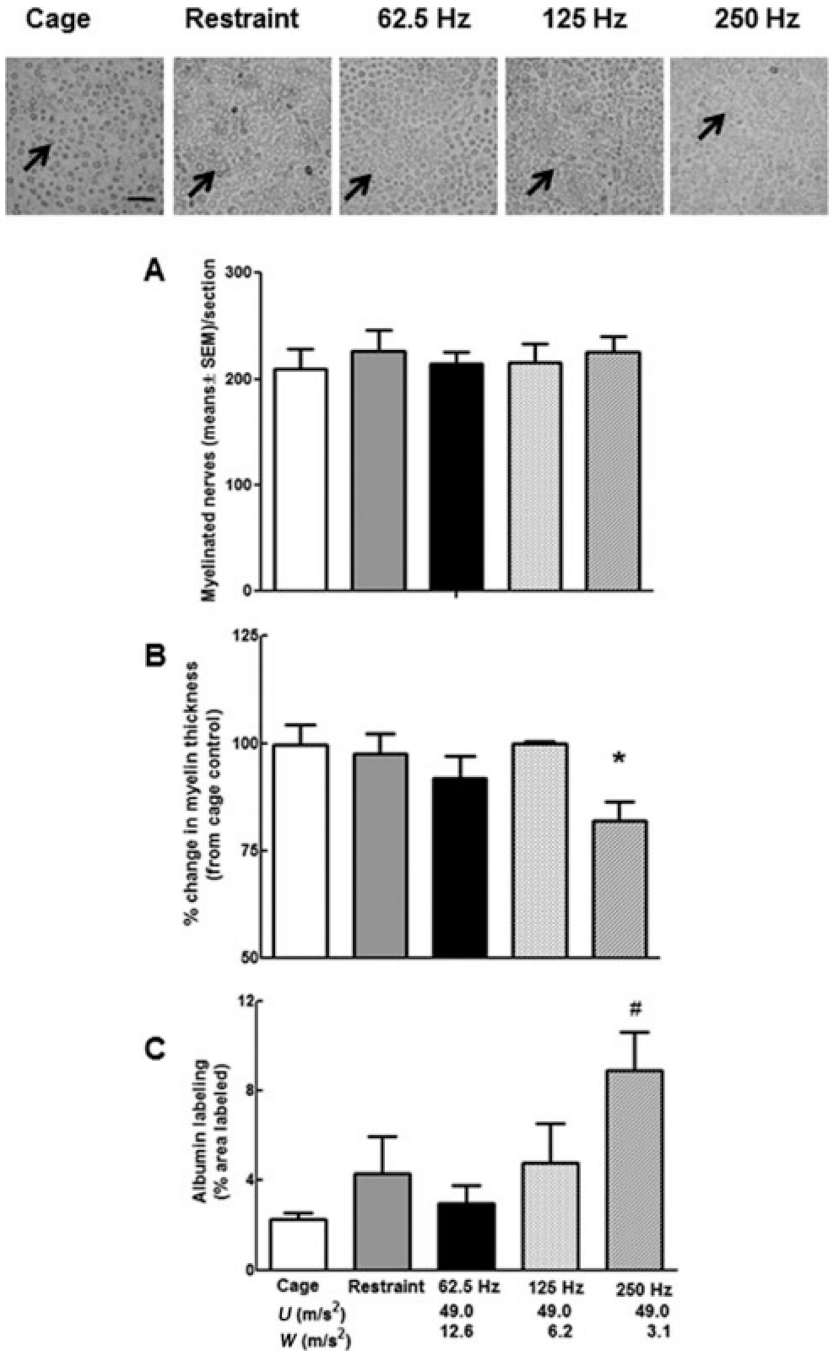

FIGURE 2.

The photomicrographs are representative photos of ventral tail nerves where the myelin has been stained with Sudan Black (arrows designate stained myelin, bar = 50 εm). The number of myelinated fibers in the sampled fields was comparable in all groups of rats (A). However, myelin thickness (B) was significantly lower in nerves collected from rats exposed to vibration at 250 Hz than in cage- or restraint-control rats (*$P < 0.05$), and the density of albumin staining (C) was higher in nerves collected from rats exposed to 250 Hz than in nerves from cage- and restraint-control rats, and rats exposed to vibration at 62.5 Hz

(#$P < 0.05$). The *x* axis shows both the unweighted acceleration (*U*) and the ISO-weighted (*W*) acceleration for each frequency.

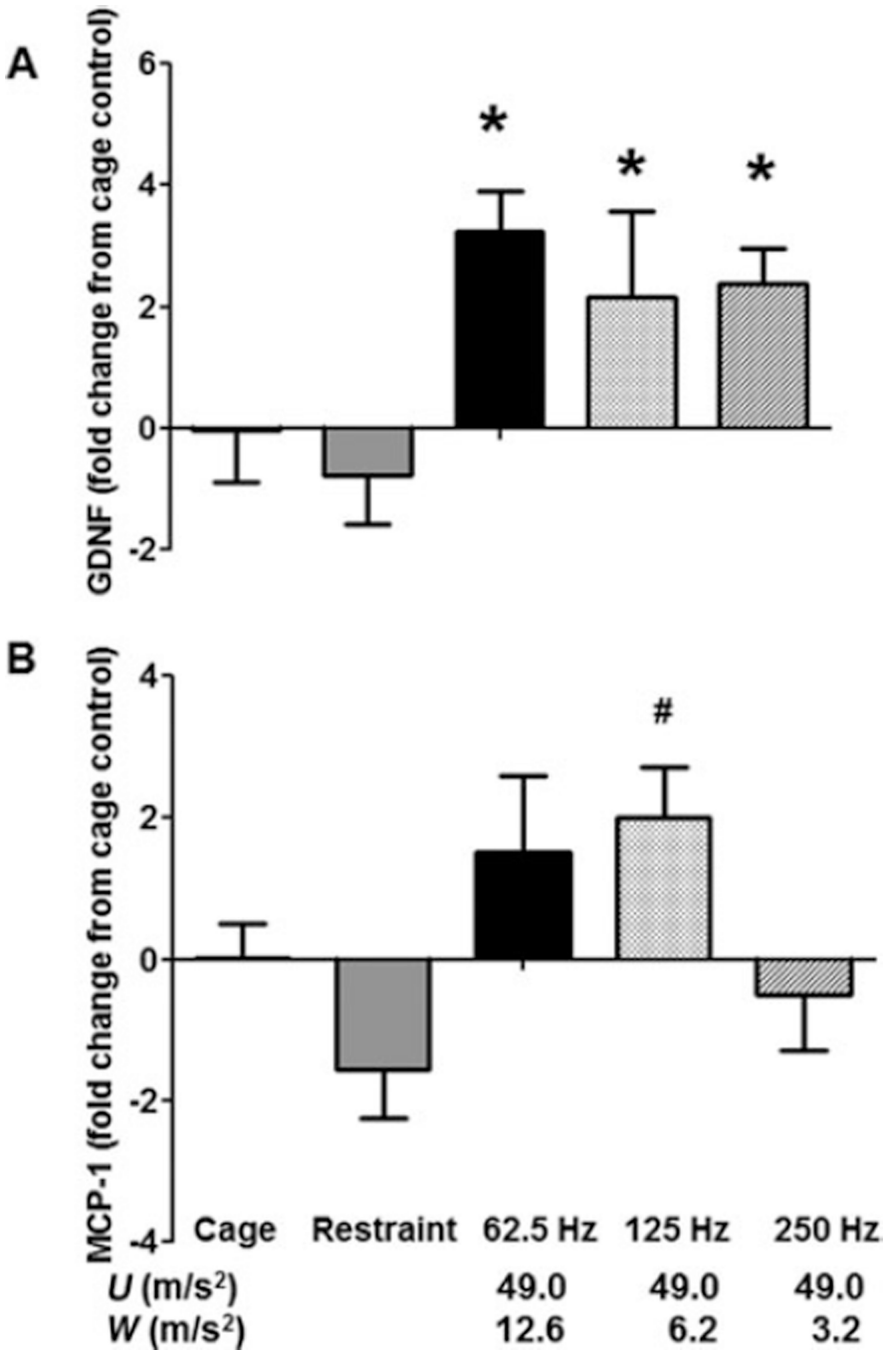

FIGURE 3.

Frequency-dependent effects of vibration on transcript levels in the ventral tail nerves. Expression of glial-derived neurotrophic factor (GDNF) was greater in nerves collected from rats exposed to vibration than in nerves collected from cage- or restraint-control rats (A; *$P < 0.05$). Monocyte chemoattractant protein (MCP)-1 transcript expression was higher in nerves collected from rats exposed to vibration at 125 Hz than in nerves from restraint-

control rats and rats exposed to vibration at 250 Hz (B; #$P < 0.05$). The *x* axis shows both the unweighted acceleration (*U*) and the ISO- weighted (*W*) acceleration for each frequency.

TABLE 1

Sequences of Primers Used for Quantitative Reverse Transcription-Polymerase Chain Reaction

Transcript	Region	NCBI Accession Number	Primer Sequence Forward; Reverse
Cadherin-2	DRG	NM_031333.1	ccatcatcgcgatacttctg; ccataccacgaacatgagga
GCH-1	Nerve	M58364	agattgcagtggccatcac; acctcgcatgaccatacaca
CYPB	DRG	AF298656.3	tggactgaggggctattcaa; ggcccatcaactgctatctt
Dynein	DRG	NM_031333.1	actggggaaagcttacaagtaca; tggccacgtgaaatccata
Elastin	DRG	NM_012722.1	ttctgggagcgtttggag; ccttgaagcataggagagacct
F-actin	DRG	AF450248.1	aagcggagggaagctttaga; ccaagtatagctggtcgatgg
GDNF	Nerve	NM_019139	ggctgtctgcctggtgtt; tcaggataatcttcgggcata
GSH-S	DRG	NM_012962	gctggacaacgagcgagt; gctgcttctcatcctgcaa
GPx-3	DRG	NM_022525	attctgggcttcccttgc; cacccggtcgaacgtact
HMOX-1	DRG	NM_012580.2	gtcaggtgtccagggaagg; ctcttccagggccgtataga
Interleukin-1β	Nerve	NM_031512	caggaaggcatgtgtcactca; aaagaaggtgcttgggtcct
Interleukin-6	Nerve/DRG	NM_012589.1	cccttcaggaacagctatgaa; acaacatcagtcccaagaagg
Keap	DRG	AF304364	cagcgtgctcgggagtat; gcagtgtgacaggttgaagaac
Lectin-1	DRG	NM_030854.1	gggaccaagcagagcatc; ctcttcatatttgactggcatga
Lumincan	DRG	NM_031050	ccttcaacacaaccagctca; ctcaagtcgaggtattcgagtg
MAPK-8	DRG	XM_341399.3	gcagccgtctcctttaggt; cattgacagacggcgaaga
MMP-9	DRG	NW_047660.1	cctctgcatgaagacgacataa; ggtcaggtttagagccacga
MCP-1	Nerve	M57441	agcatccacgtgctgtctc; gatcatcttgccagtgaatgag
MAG	Nerve	NM_017190.4	tcgcctcactgatacttcacg; ctgagttgggaatgtctcctg
MBP	Nerve/DRG	AF439750.1	ggcacgctttccaaaatct; ccatgggagatccagagc
Paf	DRG	NM_031763.3	cacgaacatgtggtagaatgc; agaagggtccaggcttgc
Psd-95	DRG	NM_019621.1	gaacacatatgacgttgtgtacctaaa; tccaggtgctgagaatacga
S100	Nerve/DRG	NM_053822.1	acgcaattaacttcgaagagttc; ccaggccagaagctctgtta
Signal transduce of Stat3	DRG	NM_012747.2	ccttggattgagagccaagat; accagagtggcgtgtgact
Soc-5	DRG	NM_001109274.1	ttacgcgcagtaggctctc; cacttcggcttcctccttc
SOD-1	DRG	NM_017050.1	taagaaacatggcggtcca; tggacacattggccacac
SOD-2	DRG	NM_017051	tggacaaacctgagccctaa; gacccaaagtcacgcttgata
TNF-α	Nerve	AJ002278	atgtggaactggcagaggag; caatcaccccgaagttcagt

CYPB, cytochrome P-450B; DRG, dorsal root ganglia; GCH-1, cyclic-GMP cyclohydrolase 1; GDNF, glial-derived neurotrophic factor; GSH-S, glutathione synthetase; GPx-3, glutatione peroxidase 3; HMOX-1, heme oxygenase 1; MAG, myelin-associated glycoprotein; MAPK-8, mitogen-activated protein kinase 8; MBP, myelin basic protein; MCP-1, monocyte chemoattractant protein 1; MMP-9, matrix metallopeptidase 9; Paf, platelet activating factor; Psd-95, postsynaptic density 95; Soc-5, sequential oligopeptide carrier 5; SOD, superoxide disumatase; TNF-α, tumor necrosis factor α.

J Occup Environ Med. Author manuscript; available in PMC 2015 December 15.

TABLE 2

Mean Fold Changes (SEM) in Transcript Levels (vs Cage Control) in the Dorsal Root Ganglia

Transcript	Cage control	Restraint control	62.5 Hz	125 Hz	250 Hz
Cadherin-2	0.1 (0.65)	0.84 (0.50)	0.62 (0.45)	0.31 (0.40)	2.08 (0.43)†
Dynein	0.01 (0.37)	1.80 (0.46)	1.19 (0.25)	0.86 (0.44)	1.52 (0.22)
Elastin	−0.80 (0.70)	1.46 (1.90)	5.75 (2.50)	1.67 (1.80)	−0.57 (1.65)
F-actin	0.02 (0.66)	1.80 (0.77)	1.14 (0.49)	0.46 (0.51)	2.10 (0.69)
G-19	0.01 (0.7)	0.52 (1.25)	−1.19 (0.65)	−0.80 (1.00)	−0.94 (0.70)
GSH-S	0.00 (0.09)	−2.43 (1.25)	0.57 (0.67)	1.56 (0.65)	3.92 (0.44)*
HMOX-1	0.00 (0.35)	−1.18 (0.76)	−1.84 (0.08)†	−1.34 (1.06)	0.27 (0.5)
Interleukin-6	0.06 (0.11)	−1.54 (0.60)	−1.68 (0.90)	−3.22 (0.90)	−4.57 (1.80)
Keap	0.10 (0.90)	2.24 (0.71)	2.98 (0.68)	1.52 (0.65)	5.22 (0.58)†
Lectin-1	0.02 (0.41)	0.44 (0.92)	0.42 (0.74)	1.03 (0.61)	2.77 (0.36)
Lumican	0.00 (0.65)	1.52 (0.85)	0.43 (0.65)	0.46 (0.36)	1.10 (0.45)
MAPK-8	0.01 (0.12)	3.23 (0.95)†	1.32 (0.44)	2.08 (0.6)	3.42 (0.56)†
MBP	0.00 (1.1)	−1.90 (1.00)	−2.21 (0.80)	−0.73 (0.52)	0.99 (0.26)
MMP-9	0.00 (1.90)	−3.49 (1.70)	−2.65 (0.76)	−4.63 (2.00)	−5.63 (1.70)
Paf	0.00 (0.45)	1.31 (0.63)	1.10 (0.38)	0.94 (0.41)	2.99 (0.36)†
Psd-96	0.00 (0.75)	1.19 (0.71)	0.48 (0.71)	0.27 (0.42)	3.23 (0.51)†
Soc-5	0.05 (0.16	1.52 (1.10)	−1.32 (0.65)	−0.27 (0.70)	0.10 (0.32)
SOD-1	0.07 (0.10)	1.45 (0.73)	−0.21 (0.27)	0.40 (0.58)	2.00 (0.55)†
SOD-2	0.00 (0.56)	1.71 (0.51)	1.63 (0.463)	1.11 (0.43)	2.95 (0.41)†
STAT3	0.00 (0.66)	−9.04 (1.4)†	−1.56 (0.60)	−5.81 (1.6)	−10.08 (1.00)†

Transcripts showing vibration-related changes in expression are highlighted. GSH-S, glutathione synthetase; HMOX-1, heme oxygenase 1; MAPK-8, mitogen-activated protein kinase 8; MBP, myelin basic protein; MMP-9, matrix metallopeptidase 9; Paf, platelet activating factor; Psd-96, postsynaptic density 96; SEM, standard error of mean; SOD, superoxide disumatase.

*Different than cage and restraint control.

†Different than cage control ($P < 0.05$).